

Numerical Simulation on Heat Transfer Phenomena in Microchannel Evaporator of A CO₂ Air Conditioning System

Ketdoan V. Chau, Tronghieu Nguyen, and Thanhtrung Dang

Department of Thermal Engineering, Hochiminh City University of Technology and Education, Vietnam

ABSTRACT: The investigation presented a numerical simulation on heat transfer behaviors in microchannel evaporator of a CO₂ air conditioning system. The conditions for numerical simulation were applied by the experimental data of a CO₂ air conditioning cycle. This cycle worked with the cooler pressure of 85 bar, evaporator pressure of 37 bar, and the CO₂ flow rate of 5.2 g/s. The temperature and pressure in microchannels are uniform; they are suitable with the theory of evaporating process. The numerical results are in good agreement with those obtained from experimental data at the same condition. In addition, the vapor quality increases from 0.50 to 0.52 when the CO₂ refrigerant enters the evaporator at position of 200mm. These results are in good agreement with experimental data.

Keywords – Numerical simulation, CO₂ refrigerant, air conditioning system, heat transfer, evaporator.

I. INTRODUCTION

The CO₂ air conditioning systems using microchannel heat exchangers are very interesting for scientists. These topics related to environmental protection and energy efficiency. Regarding to CO₂ air conditioning using microchannel evaporator, Asadi et al. [1] reviewed heat transfer and pressure drop characteristics of single and two-phase microchannels. The review showed that earlier investigations were largely concentrated using experimental methods, while more recent studies (from 2003 to 2013) used numerical simulations for predicting pressure drop and heat transfer coefficients. Huang et al. [2] also studied non-linear fluid flow and the surface temperature changes inside the microchannel with temperature sensor molecule technology. Dang et al. [3, 4] studied the microchannel heat transfer of single phase flow with water as the working fluid. The results showed that the influence of gravity to the heat transfer and pressure drop characteristics of the microchannel heat exchanger is negligible. The difference of heat transfer coefficient between the experimental method and numerical simulation is less than 9%.

Zhao et al. [5] investigated experimentally for the flow of CO₂ and R134a boiling in micro-channels, with the vapor quality is from 0.05 to 0.3. They concluded that the heat transfer coefficient of CO₂ is higher than 200% with R134a. Yun et al. [6] studied the boiling heat transfer characteristics of CO₂ in the microchannel. Results showed that the average heat transfer coefficient of CO₂ is higher than 53% with R134a. Gasche [7] investigated experimentally the evaporation of CO₂ inside the tubular microphone channel with a diameter of 0.8mm. The average heat transfer coefficient of 9700 W/(m² °C) was achieved with a standard error 35%. For the vapor quality is low (less 0.25), the slow flow is predominant; whereas, for the vapor quality is high (over 0.50), the annular flow is better. Kim and Bullard [8] researched and made a very important result for the evaporation of CO₂ refrigerant in the evaporator. In this study, the formulas of heat transfer and pressure drops due to friction for microchannel heat exchanger according to the boiling liquid and saturated vapor were mentioned from the balance mass and balances energy equations.

In the two-phase flows in microchannels, Yu et al. [9] studied two-phase gas-liquid flows in microchannels using experiment and lattice Boltzmann simulation. The results showed that the two-phase flow has more advantages on the heat transfer and transmission quality than single-phase flow. Cheng and Thome [10] researched on the evaporation temperature of CO₂ refrigerant in the micro-channel evaporator. With the two-phase flow, CO₂ heat transfer coefficient is higher and the pressure drop is lower than that of R236fa. Pettersen [11] studied about two-phase flow in microchannel tubes using CO₂ refrigerant. The results showed that the heat transfer is much influenced by the vapor quality, especially in volume flow and temperature. Thome and Ribatski [12] reviewed two-phase flow and flow boiling heat transfer and pressure drop of CO₂ in macro- and micro-channel. The review addresses flow boiling heat transfer experimental studies, macro- and

micro-scale heat transfer prediction methods for CO₂. Ducoulombier et al. [13] studied carbon dioxide flow boiling in a single microchannel. However, this study mentioned about pressure drop only.

Yun et al. [14] carried out two experiments for two-phase flow in microchannel, using R410A refrigerant. The hydraulic diameters are 1.36 and 1.44 mm. As the saturation temperatures were maintained at 0, 5 and 10 °C, the mass flux was varied from 200 to 400 kg/m²s, heat flux from 10 to 20 kW/m². However, this study did not use CO₂ as the working fluid. Cheng et al. [15] researched the updated model of CO₂ flow in the pipe diameters from 0.6 to 10 mm, mass velocities from 50 to 1500 kg /m²s, heat fluxes from 1.8 to 46 kW/m² and saturation temperatures from -28 to 25⁰C. However, studies in [14, 15] did not mention the complete CO₂ air conditioning cycle using microchannel evaporator. Schael and Kind [16] studied the flow patterns and heat transfer characteristics of CO₂ in the micro fin tube and compared with smooth pipes. The results showed that the thermal conductivity in micro-channel fins tube is significantly higher than the smooth tube.

From literature reviews above, there are no more numerical studies on heat transfer phenomena in microchannel evaporator of a complete CO₂ air conditioning system. They did not indicate phase transition of CO₂ air conditioning cycle clearly. So, it is essential to investigate heat transfer phenomena on microchannel evaporator of a CO₂ air conditioning system by using numerical simulation.

II. METHODOLOGY

2.1 Mathematical Model

The governing equations describing the microchannel evaporator consist of the continuity equation, momentum equations, and energy equation [3, 15, 16].

Fluid properties equations in 3D Cartesian coordinates can be shown by:

$$\rho(u.\nabla)u =$$

$$\nabla.\left[-pI + (\mu + \mu_T)(\nabla u + (\nabla u)^T) - \frac{2}{3}(\mu + \mu_T)(\nabla.u)I - \frac{2}{3}\rho kI\right] + F$$

$$\nabla.(\rho u) = 0$$

$$\rho(u.\nabla)k = \nabla.\left[\left(\mu + \frac{\mu_T}{\sigma_k}\right).\nabla k\right] + p_k - \rho\varepsilon$$

$$\rho(u.\nabla)\varepsilon = \nabla.\left[\left(\mu + \frac{\mu_T}{\sigma_\varepsilon}\right).\nabla\varepsilon\right] + C_{e1}\frac{\varepsilon}{K}P_k - C_{e2}\rho\frac{\varepsilon^2}{K}, \varepsilon = ep$$

$$\rho C_p u.\nabla T + \nabla.q = Q + Q_p + Q_{vd}$$

$$q = -k.\nabla T$$

Equations for solid can be shown by:

$$\rho C_p u.\nabla T + \nabla.q = Q + Q_{ted}$$

$$q = -k.\nabla T$$

Equations for change phase can be shown by:

$$\rho C_p u.\nabla T + \nabla.q = Q + Q_p + Q_{vd}$$

$$q = -k.\nabla T$$

$$\rho = \theta\rho_{phase1} + (1-\theta)\rho_{phase2}$$

$$C_p = \frac{1}{\rho}\left(\theta\rho_{phase1}C_{p,phase1} + (1-\theta).\rho_{phase2}C_{p,phase2}\right) + L\frac{\partial\alpha_m}{\partial T}$$

$$K = \theta k_{phase1} + (1-\theta)K_{phase2}$$

$$\alpha_m = \frac{1}{2}\frac{(1-\theta)\rho_{phase2} - \theta\rho_{phase1}}{\theta\rho_{phase1} + (1-\theta)\rho_{phase2}}$$

Equations for wall:

$$u.n = 0$$

$$\left[(\mu + \mu_T)(\nabla_u + (\nabla u)^T) - \frac{2}{3}(\mu + \mu_T)(\nabla.u)I - \frac{2}{3}\rho kI \right] n = -\rho \frac{u_\tau}{\delta_w^+} u_{tang}$$

$$u_{tang} = u - (u.n)n$$

$$\nabla k.n = 0, \varepsilon = \rho \frac{C_\mu k^2}{K_v \delta_w^+ \mu}$$

Equations for inlet:

$$-\int_{\partial.\Omega} \rho(u.n)d_{bc}dS = m$$

$$k = \frac{3}{2}(U_{ref} / T)^2, \varepsilon = C_\mu^{3/4} \frac{k^{3/2}}{L_T}$$

Equations for outlet:

$$\left[-pl + (\mu + \mu_T)(\nabla u + (\nabla u)^T) - \frac{2}{3}(\mu + \mu_T)(\nabla.u).I - \frac{2}{3}\rho kI \right] n = -p_o n$$

$$\nabla k.n = 0, \nabla \varepsilon.n = 0$$

$$-nq = \rho C_p C_\mu^{1/4} k^{1/2} \frac{T_w - T}{T^+}$$

Initial conditions for temperature:

$$T = T_0$$

Initial conditions for heat flux:

$$-n.q = q_0$$

where p is pressure, p_o is pressure at the outlet, u is velocity field, T is temperature, Q is heat transfer rate, Q_i is internal heat generation, k is thermal conductivity, μ is dynamic viscosity, ρ is density, u is velocity in the x-direction, v is velocity in the y-direction, w is velocity in the z-direction, q is heat flux, c is specific heat, m is mass flow rate, S is area, k is turbulent kinetic energy, n is normal vector, ε is turbulent dissipation rate, u_{tang} is velocity field, L_T is turbulence length scale, l_T is Turbulent intensity, U_{ref} is is velocity Reference, K is Average viscous stress, α is thermal diffusivity and θ is phase indicator.

2.2 Design and numerical simulation

The heat transfer process of this microchannel evaporator is carried out between the CO₂ refrigerant and air. Fig. 1 shows the dimensions of the evaporator. The material for this heat exchanger is aluminum, used as a substrate with the thermal conductivity of 237 W/(m°C), density of 2,700 kg/m³, and specific heat at constant pressure of 904 J/(kg°C).

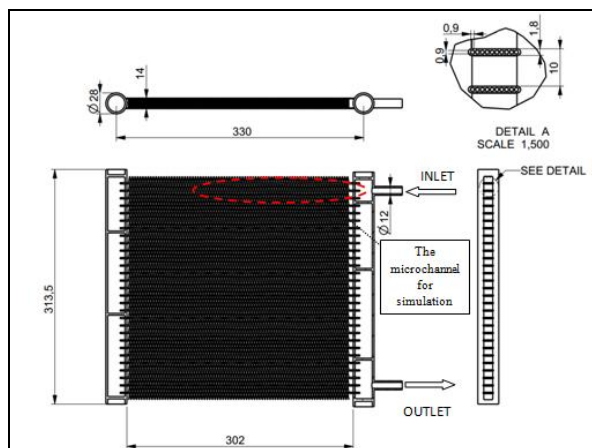


Fig. 1 Dimensions of the microchannel evaporator

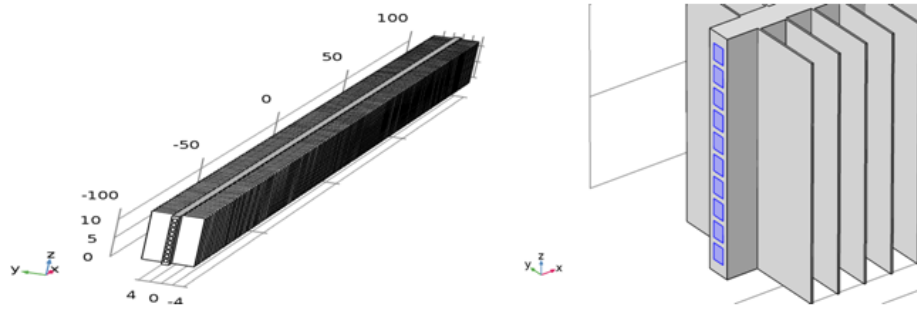


Fig. 2 Dimensions of the microchannel section for simulation

The evaporator has six passes (29 channels in the total). Microchannels have a square cross-section with the side of 900 μm . The total heat transfer area of this evaporator is 2.5 m^2 . To simplify the numerical simulation for the microchannel evaporator, the sample for simulation is the microchannel section from the inlet of evaporator to the position of 200 mm, as indicated in Fig.1. The dimensions of the microchannel section for simulation are shown in Fig.2.

Numerical study of the behavior of the microchannel section of evaporator with 3D was done by using the COMSOL Multiphysics software, version 5.2a. The mesh diagram of the microchannel section of evaporator is shown in Fig.3. The nodalization of this model was done by using 244329 mesh elements. The solution time of this model was 1505 seconds; the number of degrees of freedom was 287833 (plus 58627 internal DOFs); a relative tolerance was 10^{-6} .

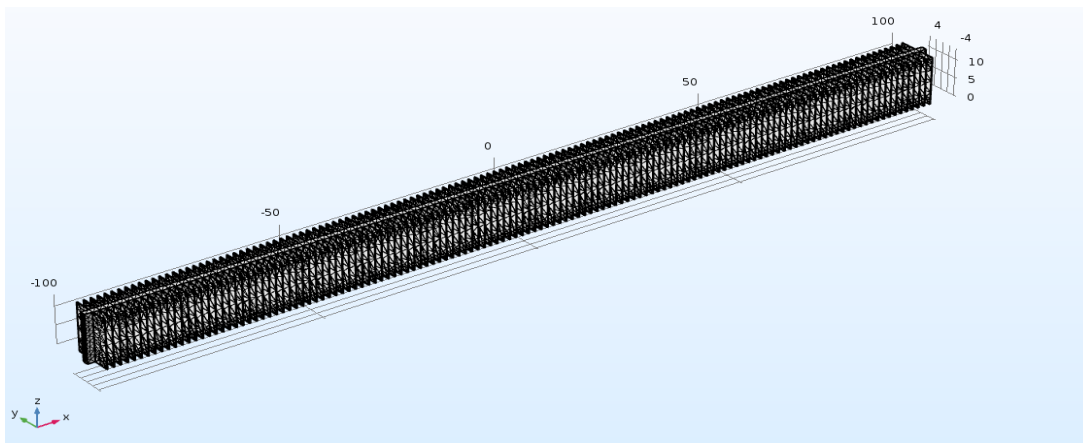


Fig. 3 Grid mesh diagram of the microchannel section of evaporator

III. RESULTS AND DISCUSSION

The simulation conditions were based on the thermodynamic parameters of the CO_2 air conditioning system in Fig. 4. The principle of CO_2 air conditioning cycle was indicated in [17].

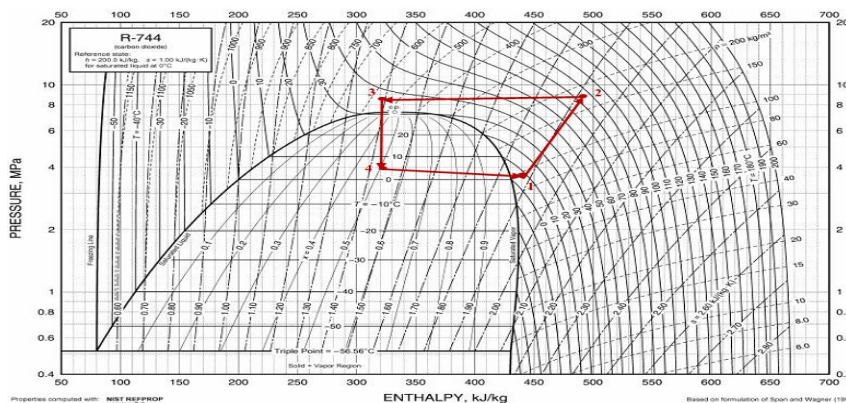


Fig. 4 The thermodynamic points of the cycle on p-h diagram

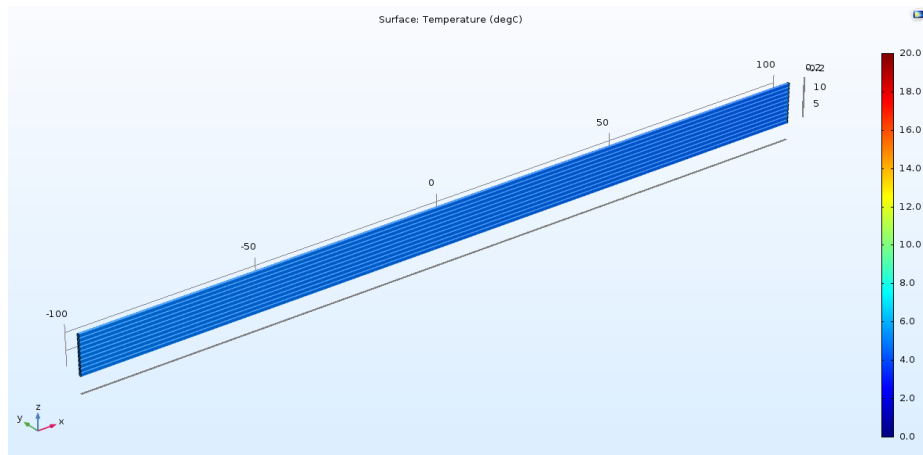


Fig. 5 Temperature profiles of the microchannel section of the evaporator

This cycle operated with the cooler pressure of 85 bar, evaporator pressure of 37 bar (corresponding with the evaporating temperature of 5 °C), and the CO₂ flow rate of 5.2 g/s. The numerical results in Fig. 5 show temperature profiles of the microchannel section. It is observed that the temperature in microchannels is uniform; it is suitable with the theory of evaporating process. The numerical results in Fig. 5 are in good agreement with those obtained from experimental data at the same condition (as shown in Fig. 6).

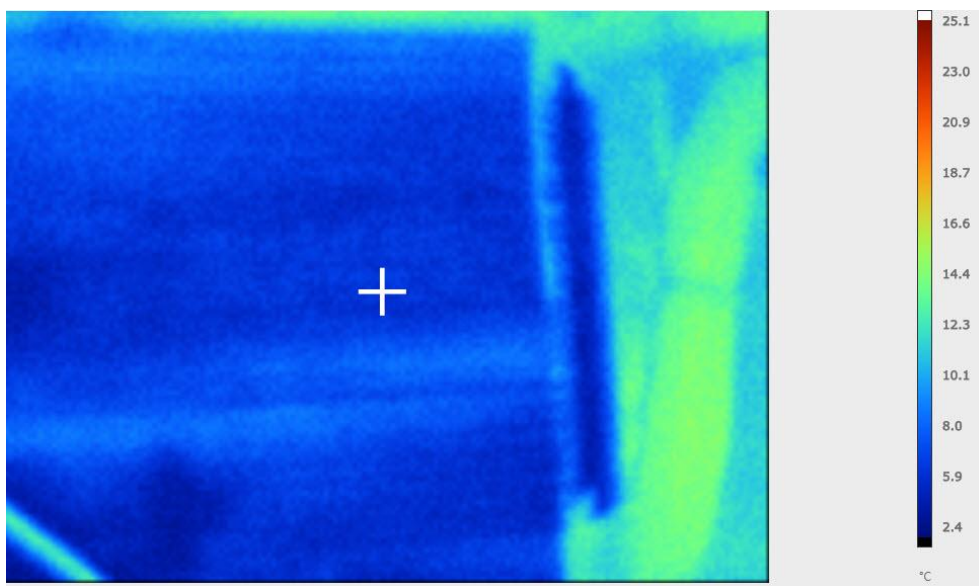


Fig. 6 A picture of microchannel evaporator using thermal camera

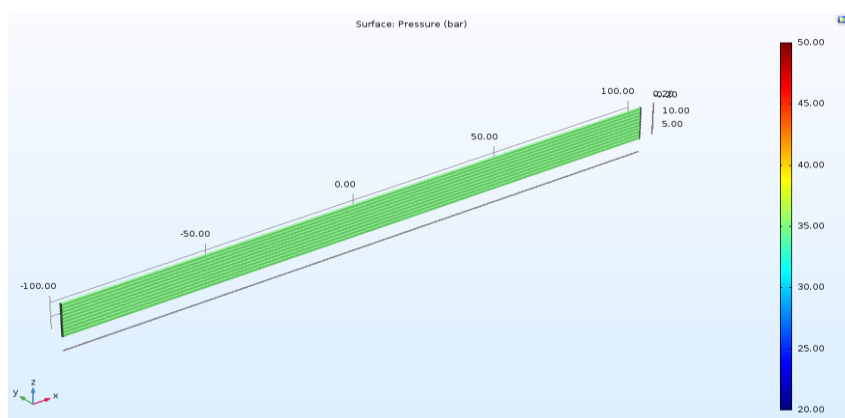


Fig. 7 Pressure profiles of the microchannel section of the evaporator

The pressure profiles of microchannel section of evaporator are shown in Fig. 7. The pressure value in microchannels is also uniform with the values around 37 bar; it also is suitable with the theory of evaporating process. The numerical results in Fig. 7 are in good agreement with those obtained from experimental data in Fig. 4. However, in Fig. 4, the pressures at the outlets of the evaporator are lower than those obtained from the inlet ones. It is due to pressure drop of the heat exchanger and suction force of the compressor. In this experiment, the liquid and flash refrigerant had the vapor quality of 0.5; this value was used to simulate. The numerical results in Fig. 8 show the phase change in the microchannels. It is observed that the vapor quality increases from 0.50 to 0.52 when the CO₂ refrigerant enters evaporator at position of 200mm. These results are in good agreement with experimental data (the experimental data of vapor quality at the position of 200 mm was estimated about 0.53). It is noted that the results in Figs. 5-8 have rarely seen in literature reviews. These numerical results will be valuable to investigate the evaporation and condensation in microchannels, especially for CO₂ refrigerant.

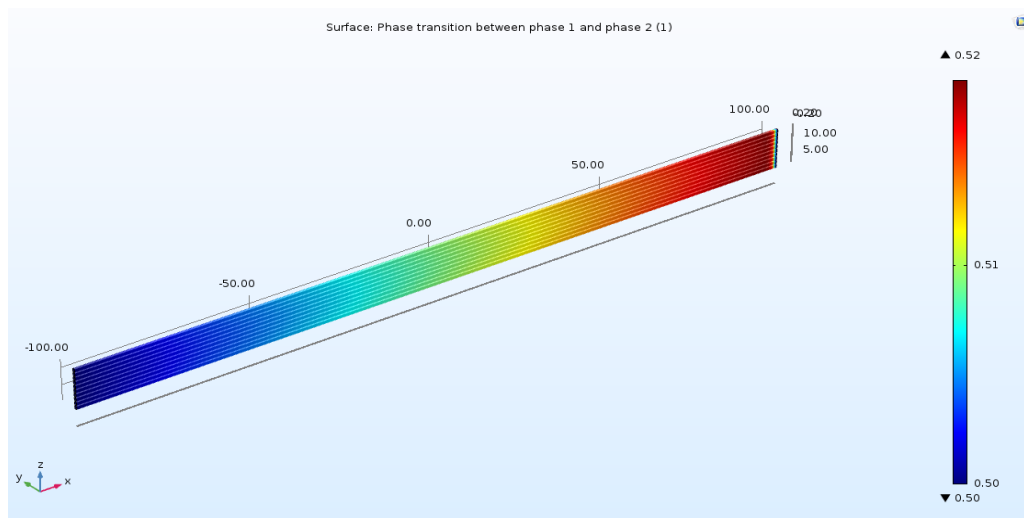


Fig. 8 Phase transition in the microchannels

IV. CONCLUSION

A numerical simulation on heat transfer behaviors in microchannel evaporator of a CO₂ air conditioning system was done. The numerical results were compared with experimental data of a CO₂ air conditioning cycle. This cycle operated with the cooler pressure of 85 bar, evaporator pressure of 37 bar (corresponding with the evaporating temperature of 5 °C), and the CO₂ flow rate of 5.2 g/s.

The temperature and pressure in microchannels are uniform; they are suitable with the theory of evaporating process. The numerical results of temperature and pressure are in good agreement with those obtained from experimental data at the same condition.

In this study, the vapor quality increases from 0.50 to 0.52 when the CO₂ refrigerant enters evaporator at position of 200 mm. These results are in good agreement with experimental data. It is noted that the numerical results have rarely seen in literature reviews.

ACKNOWLEDGEMENTS

The supports of this work by the project No.B2015.22.01 (sponsored by Vietnam Ministry of Education and Training) are deeply appreciated.

REFERENCES

- [1] Masoud Asadi, Gongnan Xie, Bengt Sundén, A review of heat transfer and pressure drop characteristics of single and two-phase microchannels, *International Journal of Heat and Mass Transfer*, 79, 2014, 34–53.
- [2] Chih-Yung Huang, Cheng-Min Wu, Ying-Nung Chen, Tong-Miin Liou, The experimental investigation of axial heat conduction effect on the heat transfer analysis in microchannel flow, *International Journal of Heat and Mass Transfer*, 70, 2014, 169–173.
- [3] Thanhtrung Dang, Jyh-tong Teng, Jiann-cherng Chu, A study on the simulation and experiment of a microchannel counter-flow heat exchange, *Applied Thermal Engineering*, 30, 2010, 2163-2172.
- [4] Thanhtrung Dang, Jyh-tong Teng, The effects of configurations on the performance of microchannel counter-flow heat exchangerse - An experimental study, *Applied Thermal Engineering*, 31, 2011, 3946-3955.
- [5] Xiumin Zhao, P.K. Bansal, Flow boiling heat transfer characteristics of CO₂ at low temperatures, *International Journal of Refrigeration*, 30, 2007, 937-945.
- [6] Rin Yun, Yongchan Kim, Min Soo Kim, Convective boiling heat transfer characteristics of CO₂ in microchannel, *International Journal of Heat and Mass Transfer*, 48, 2005, 235–242.

- [7] José L. Gasche , Carbon Dioxide Evaporation in a Single Microchannel, *Journal of the Brazilian Society of Mechanical Sciences*, 28 (1), 2006.
- [8] Man-Hoe Kim, Clark W. Bullard, Development of a microchannel evaporator model for a CO₂ air-conditioning system, *Energy*, 26, 2001, 931–948.
- [9] Zhao Yu, Orin Hemminger, Liang-Shih Fan, Experiment and lattice Boltzmann simulation of two-phase gas–liquid flows in microchannels, *Chemical Engineering Science*, 62, 2007, 7172 – 7183.
- [10] Lixin Cheng, John R. Thome, Cooling of microprocessors using flow boiling of CO₂ in a micro-evaporator: Preliminary analysis and performance comparison, *Applied Thermal Engineering*, 29, 2009, 2426–2432.
- [11] Jostein Pettersen, Flow vaporization of CO₂ in microchannel tubes, *Experimental Thermal and Fluid Science*, 28, 2004, 111–121.
- [12] John R. Thome, Gherhardt Ribatski, State-of-the-art of two-phase flow and flow boiling heat transfer and pressure drop of CO₂ in macro- and micro-channel, *International Journal of Refrigeration*, 28, 2005, 1149–1168.
- [13] Maxime Ducoulombier , Stéphane Colasson, Jocelyn Bonjour, Philippe Haberschill, Carbon dioxide flow boiling in a single microchannel – Part I: Pressure drop, *Experimental Thermal and Fluid Science*, 35, 2011, 581–596.
- [14] R. Yun, J.Y. Heo, Y. Kim, Evaporative heat transfer and pressure drop of R410A in microchannels, *International Journal of Refrigeration*, 29, 2006, 92-100.
- [15] Lixin Cheng, Gherhardt Ribatski, Jesús Moreno Quibén, John R. Thome, New prediction methods for CO₂ evaporation inside tubes: Part I – A two-phase flow pattern map and a flow pattern based phenomenological model for two-phase flow frictional pressure drop, *International Journal of Heat and Mass Transfer*, 51, 2008, 111–124.
- [16] Arndt-Erik Schael, Matthias Kind, Flow pattern and heat transfer characteristics during flow boiling of CO₂ in a horizontal micro fin tube and comparison with smooth tube data, *International Journal of Refrigeration*, 28, 2005, 1186–1195.
- [17] Tankhuong Nguyen, Tronghieu Nguyen, Thanhtrung Dang, and Minhung Doan, An experiment on a CO₂ air conditioning system with Copper heat exchangers, *International Journal of Advanced Engineering, Management and Science*, Vol. 2, 2016, 2058-2063.